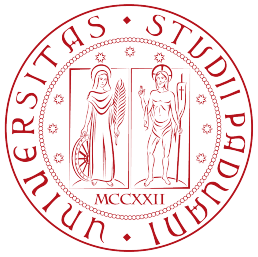

Università degli Studi di Padova

Dipartimento di Fisica e Astronomia G.Galilei

Corso di Laurea Triennale in
Fisica

Quantum optimal control of two-qubit gates in Rydberg atoms

Relatore:
Prof. Simone Montangero

Laureando:
Marco Dall'Ara
1217301

Anno Accademico 2021/2022

Abstract

Quantum computers promise to outperform conventional computational processes by taking advantage of exclusive quantum properties, such as superposition and entanglement. In the last years, several breakthroughs have demonstrated Rydberg atoms as a promising scalable quantum computing platform. Rydberg atoms are excited atoms that show exaggerated properties, where two different internal states encode a qubit with long coherence times. The progress in manipulating individual Rydberg atoms has allowed the experimental realization of single and two-qubit gate protocols. This has motivated a widespread theoretical interest in improving gate fidelity and finding alternative protocols. After reviewing the physics of Rydberg atoms and the most up-to-date gate protocols, in this Thesis we simulate one and two qubits gates, then we apply optimal control techniques, as implemented in the open-source optimal control suite QuOCS, to optimize the laser pulse shapes for the realization of controlled-phase gate.

Contents

Introduction

In the last 70 years, physicists have extensively used simulation on classical computers to further investigate nature laws. However, the complexity of simulating quantum systems in classical digital computers scales exponentially with the number of its sub-constituents. Richard Feynman proposed for the first time to solve this problem by implementing the simulation in a quantum computer [1]: a device that works with qubits as elementary units of information. Beyond chemical-physical simulations, examples as the Shor algorithm [2] and the Quantum Fourier Transform [3] have made clear the huge potential of quantum computers. One way to define a quantum computation algorithm is with a quantum circuit composed of quantum logic gates. In complete analogy with classical computers, there exist universal sets of quantum gates from which we can realize every algorithm. It can be proven that the combination of single-qubit gates plus entangling operations realizes a universal set of quantum gates [4].

Quantum computers based on neutral atoms trapped in optical tweezers and manipulated with laser pulses are a promising technology. The advantages of this platform are the long lifetime of the qubits since they are encoded onto hyperfine ground states of neutral atoms, and scalability, as long as many atoms can be packed close together given the weak interaction between neutral atoms in the array. In the early 2000s, it has been proposed to realize a two-qubit operation by temporarily exciting neutral atoms to Rydberg states [5]. Indeed, when atoms get excited in Rydberg states they became much larger and with a huge electric dipole moment. The latter makes Rydberg states interact very strongly with each other. More specifically, the strong interaction permits a peculiar effect called Rydberg blockade for which more than an atom cannot be excited to the Rydberg state at the same time, and that enables the entangling between qubits [6]. This discovery with the experimental proof of optical tweezers platform [7], kicked off neutral atoms as quantum hardware shortening the gap in gate fidelities with respect to ions and superconductive circuit implementations [8].

To be able to execute efficiently quantum algorithms, the current main task of quantum computing is to improve gate quality. Several engineering techniques are then being applied to manipulate quantum systems. One of them is quantum optimal control [9], a family of algorithms to find the optimal pulse shape to improve quantum technologies via a minimization of a figure of merit.

The aim of this Thesis is to analyze different protocols that implement a controlled-phase gate in a neutral atoms platform. Our simulations neglect Rydberg states' decay and other contribution to the dynamics, and then we do not expect to find realistic fidelities. Then, our goal is to minimize the gate time reducing the average time spent on Rydberg states. Indeed,

as been shown in Ref. [10], the latter is the biggest source of intrinsic errors for these kind of gates. Firstly, we reproduce a protocol with two laser pulses of length τ, phase jump ξ, and constant detuning Δ, in the hypothesis of a perfect blockade, as in Ref. [8]. We optimize the detuning and the gate time with a direct search method in the imperfect blockade regime analyzing the effect of a finite interaction on the gate time. Then, by following the approach of Ref. [11], we make use of optimal control techniques to reduce the total time of the gate. In this case, we consider a symmetric detuning pulse with a zero phase and we perform the optimization by using the dCRAB algorithm implemented in the software QuOCS [12].

In Chapter 1, we briefly describe the physics of Rydberg atoms. Firstly, we summarize the general properties of individual Rydberg atoms as their long coherence times or their huge electric dipole moment. Then, we describe the interaction between two Rydberg atoms and how atoms can be manipulated using light. Afterwards, we introduce the phenomenon of the Rydberg blockade, arising from to the strong interaction between Rydberg states. As we have already mentioned, the Rydberg blockade phenomenon plays an important role in gate protocols, making possible entangling operations in a neutral atom system. In Chapter 2, we give a brief introduction to quantum optimal control theory. We focus our attention on the dressed Chopped Random Basis (dCRAB) technique: an optimization algorithm to compute the optimal pulse to let the system evolve from an initial state to a target state.

Finally, in Chapter 3, we review some protocols to realize one- and two-qubit gates with Rydberg atoms. We show how a controlled-phase gate can be realized by using different input pulse shapes and how to optimize it with quantum optimal control techniques.

Chapter 1

Rydberg atoms physics

Rydberg atoms are atoms with a valence electron in a highly-excited state, i.e. states with large principal quantum number n. Since almost all of their parameters scale with positive powers of n they show exaggerated proprieties, and that is exploited in quantum technologies [13]. For example, Rydberg atoms have long decoherence times, that scales as n^3. Furthermore, they are huge and their interaction is really strong since size and electric dipole moment scale as n^2. The strong interaction between Rydberg atoms enables a phenomenon called Rydberg blockade. This effect prevents the simulateneous excitation to a specific Rydberg state of more than an atom in a certain volume and can be exploited to entangle several qubits [14].

In Sec. 1.1, we briefly explain the general properties of the Rydberg atoms and their scaling behavior with the principal quantum number n. Then, in Sec. 1.2 and in Sec. 1.3 we describe the interaction between two Rydberg atoms and we explain the interaction with an atom with an external electromagnetic field. Finally, in Sec 1.4 we focus on the Rydberg Blockade mechanism.

1.1 General properties

In the simplest approach, it is sufficient to treat Rydberg atoms as hydrogenic. Indeed, the orbit size $\bar{r}$ of Rydberg atoms scales with n^2, and then the outer electron stays far away from the atomic core and in a first approximation one can assume that all the electrons of the inner states shield the nucleus [14]. For a more realistic model, one should take into account relativistic effects and spin-orbit interaction: the so-called fine structure correction [15]. Furthermore, we can consider a non-perfect shield of the ionic nucleus, introducing the quantum defect theory [6]. From a semi-classical point of view, as we show in Fig. 1.1a, the quantum defect theory correction needs to be introduced for states with angular momentum l far from n, since the outer electron is close to the ionic nucleus only at some point. This is still valid in quantum mechanics as shown with an example about Rubidium atoms in Fig. 1.1b. The corrected Hamiltonian eigenvalues are given by $E_{n,l} = E'_{n,l} + \Delta E_{fs}$ where ΔE_{fs} is called *fine structure correction* [15] :

$$\Delta E_{fs} = E_n^0 \frac{\alpha^2}{n^2}\left[\frac{n}{j+1/2} - \frac{3}{4}\right], \tag{1.1}$$

The term $E'_{n,l}$ takes into account quantum defect theory [6] :

$$E'_{n,l} = -\frac{R_\infty}{1+\dfrac{m_e}{M}}\frac{1}{(n-\delta_{n,l})^2}\ , \tag{1.2}$$

where E_n^0 are the energies of the hydrogen atom, n is the principal quantum number, l is the azimuthal quantum number, α is the fine structure constant, R_∞ is the Rydberg constant, m_e is the mass of the electron, M is the total mass of the atom, j is the total angular momentum quantum number and $\delta_{n,l}$ is the quantum defect which depends on the atomic species and on n and l.

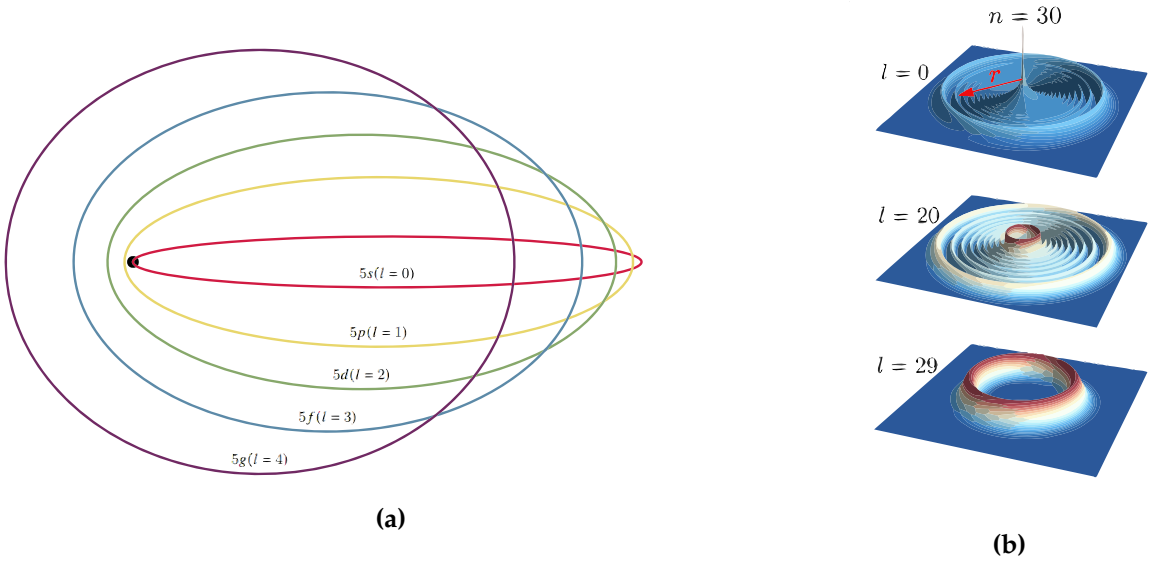

(a) **(b)**

Figure 1.1: (a) Semiclassical orbiting of the valence electron around the atomic core(black dot), with l orbital angular momentum and principal quantum number $n = 5$. For lower l, the outer electron is close to the ionic core and thus the perfect-shield hypothesis should be corrected with quantum defect theory. (b) Density distributions of the valence electron in the radial direction of 87Rb [14]. When l=n-1 this electron is highly localized around $n^2 a_0$, indeed we are in the perfect-shield regime.

Rydberg atoms have a lifetime τ that has essentially two contributions:

$$\frac{1}{\tau} = \frac{1}{\tau_0} + \frac{1}{\tau_{bb}} \,. \tag{1.3}$$

The radiative lifetime τ_0 takes into account spontaneous emission and scales as n^3 for final low energy states and as n^5 to neighboring Rydberg states. Instead, the blackbody lifetime τ_{bb} considers the coupling between the atom and the blackbody radiation in the environment and scales as n^2 [14].

1.2 Rydberg-Rydberg interaction

Let us consider two Rydberg atoms separated by a distance R. If the interatomic distance of two Rydberg atoms is much greater than the Rydberg state radius, we can describe our atoms as electric dipoles with $\mathbf{p} = -e\mathbf{d}$, where d is the displacement between the electron and the

ionic nucleus. Then atoms interaction reduces to a dipole-dipole interaction [16]:

$$V_{dd} = \frac{e^2}{4\pi\epsilon_0}\frac{\mathbf{d}_1\cdot\mathbf{d}_2 - 3(\mathbf{d}_1\cdot\hat{\mathbf{u}}_R)(\mathbf{d}_2\cdot\hat{\mathbf{u}}_R)}{|\mathbf{R}|^3}\ , \tag{1.4}$$

where $\mathbf{R}$ is the interatomic distance and $\hat{\mathbf{u}}_R$ the versor along $\mathbf{R}$.
Without an external electric field, by indicating a general eigenvector with $|\Psi_{nlm}\rangle$ and the parity operator with $\hat{P}$, it is easy to show that $\overline{\mathbf{d}} = 0$ since for each eigenvector we have

$$\begin{aligned}\overline{\mathbf{d}}_{nlm} &:= \langle\Psi_{nlm}|\ \mathbf{d}(t)|\Psi_{nlm}\rangle = \langle\Psi_{nlm}(t)|\mathbf{d}|\Psi_{nlm}(t)\rangle = \langle\Psi_{nlm}|\mathbf{d}|\Psi_{nlm}\rangle \\ &= \langle\Psi_{nlm}|\hat{P}\hat{P}^{-1}\mathbf{d}\hat{P}\hat{P}^{-1}|\Psi_{nlm}\rangle = \langle\Psi_{nlm}|\hat{P}(-\mathbf{d})\hat{P}^{-1}|\Psi_{nlm}\rangle = -\overline{\mathbf{d}}_{nlm}\ ,\end{aligned} \tag{1.5}$$

and then $\overline{\mathbf{d}} = 0$ which involves that $\overline{V_{dd}} = 0$.

Beside that, $\mathbf{d}$ has non-zero matrix elements between states with different parities, so it can be shown that in the case of a single transition from $|r_1\rangle|r_2\rangle$ to $|r_1'\rangle|r_2'\rangle$, where each one of them is a different Rydberg state, we can reduce the description with an Hamiltonian in the subspace $\{|r_1\rangle|r_2\rangle, |r_1'\rangle|r_2'\rangle\}$ [14]:

$$\hat{H} = \begin{bmatrix} 0 & C_3/R^3 \\ C_3/R^3 & \delta_F \end{bmatrix}\ , \tag{1.6}$$

where $C_3 \propto n^4$ is the anisotropic interaction coefficient and $\delta_F = (E_{r_1'} + E_{r_2'}) - (E_{r_1} + E_{r_2})$ the Foster defect. In the case where $\delta_F \gg V(R) := C_3/R^3$ we could treat the system with perturbation theory getting as a result $\Delta E_\pm = \pm C_6'/R^6$ with $C_6' = C_3^2/\delta_F$. Note that, since $\overline{V_{dd}} = 0$ we need to consider second-order corrections.

By fixing $r_1 = r_2 = r$, we can generalize and consider all the second-order perturbations of others Rydberg states:

$$C_{rr} = \sum_{|r_1'\rangle|r_2'\rangle}\left[\frac{C_3^2}{R^6\delta_F}\right]_{|r\rangle|r\rangle->|r_1'\rangle|r_2'\rangle} = \sum_{|r_1'\rangle|r_2'\rangle}\frac{|\langle r_1', r_2'|V_{dd}|r, r\rangle|^2}{2E_r - E_{r_1'} - E_{r_2'}} = C_{6,rr}/R^6\ . \tag{1.7}$$

This is the so-called Van der Waals interaction [17], and we will consider that as the Rydberg-Rydberg interaction in the next chapters. The $C_{6,rr}$ coefficient scales as n^{11} which shows the huge interactions between Rydberg atoms.

1.3 Light-Atom interaction

Let us consider a two-level atom with ground state $|g\rangle$ and excited state $|e\rangle$ interacting with an electric field. We describe the oscillating electric field as a monochromatic plane wave $\mathbf{E}(t) = \mathbf{E}_0'\cos(\omega t + \phi) = \mathbf{E}_0 e^{-i\omega t} + \mathbf{E}_0^* e^{i\omega t}$ with $\mathbf{E}_0 = \mathbf{E}_0' e^{i\phi}/2$. The interaction between the atom and the light can be modeled as:

$$\hat{H}_{int} = -\mathbf{p}\cdot\mathbf{E}(t)\ , \tag{1.8}$$

where $\mathbf{p}$ is the electric dipole of the atom. In this description, we are considering the atom as a dipole and we are neglecting higher multipole terms since their smaller contributions. As we have seen in Eq. (1.5) the dipole operator has only non-diagonal terms different by zero, and then the Hamiltonian of the two level system with the interaction of the dipole with the light is:

$$\hat{H}_{int} = -\hbar(\Omega e^{-i\omega t} + \hat{\Omega} e^{i\omega t}) |g\rangle \langle e| - \hbar(\hat{\Omega}^* e^{-i\omega t} + \Omega^* e^{i\omega t}) |e\rangle \langle g| \ , \tag{1.9}$$

with $\Omega_0 = \hbar^{-1} \langle e|\mathbf{p}|g\rangle \cdot \mathbf{E}_0'$ the Rabi frequency, $\Omega = -\frac{\Omega_0}{2} e^{-i\phi}$ and $\hat{\Omega} = -\frac{\Omega_0}{2} e^{i\phi}$. Defining $\omega_d := \omega_{|e\rangle} - \omega_{|d\rangle}$ we can express the Hamiltonian of the non-interacting system as $\hat{H}_0 = -\hbar\omega_d/2 |g\rangle \langle g| + \hbar\omega_d/2 |e\rangle \langle e|$ since the difference of the two eigenvalues of the energies are $\Delta E = E_e - E_g$. The total Hamiltonian is then

$$\hat{H} = \hat{H}_0 + \hat{H}_{int} \ . \tag{1.10}$$

If we consider a unitary transformation to the Dirac picture we get

$$\hat{H}_{int,dirac} = -\hbar(\Omega e^{-i\Delta t} + \hat{\Omega} e^{i(\omega_d+\omega)t}) |g\rangle \langle e| - \hbar(\hat{\Omega}^* e^{-i(\omega_d+\omega)t} + \Omega^* e^{i\Delta t}) |e\rangle \langle g| \ . \tag{1.11}$$

Setting the electric field near resonance we have that the detuning $\Delta := \omega - \omega_d$ satisfy $\Delta \ll \omega_d + \omega$, the so-called rotating wave approximation [18]. Then, in Equation (1.11) the terms with frequency $\omega_d + \omega$ oscillates much faster with respect to the other and then we can neglect it:

$$\hat{H}_{int,dirac} \approx -\hbar(\Omega e^{-i\Delta t}) |g\rangle \langle e| - \hbar(\Omega^* e^{i\Delta t}) |e\rangle \langle g| \ . \tag{1.12}$$

Finally, transforming back to the Schrodinger picture and going in a rotating frame of reference defined by $\hat{H}_{rwf} = \hat{U}\hat{H}\hat{U}^\dagger + i\hbar\frac{\partial \hat{U}}{\partial t}\hat{U}^\dagger$, with

$$\hat{U} = \begin{bmatrix} e^{-i\omega t/2} & 0 \\ 0 & e^{i\omega t/2} \end{bmatrix} \ , \tag{1.13}$$

we get the Hamiltonian in the rotating frame,

$$\hat{H} = -\hbar\Delta |e\rangle \langle e| + \hbar(\Omega |e\rangle \langle g| + \Omega^* |g\rangle \langle e|) \ . \tag{1.14}$$

Note that we have not considered the spatial term of the electric wave, as if it is interacting with the atoms in a single point fixed to zero.

1.4 Rydberg blockade effect

Now, let us consider two identical Rydberg atoms both interacting with light, where each one has a basis composed of a ground state $|g\rangle$ and a Rydberg state $|r\rangle$. Moreover, we consider a resonant laser that couples $|g\rangle$ to $|r\rangle$. Since we are using resonant light, we shrink all the possible Rydberg states only to $|r\rangle$, but we do not neglect the interaction of all Rydberg states

with the only one reachable. Due to the Rydberg-Rydberg interaction, we cannot promote both atoms as the first excited shifts the Rydberg energy level of the other off-resonance. The dynamic is then governed by the following Hamiltonian:

$$\hat{H} = \hbar(\Omega \left|r\right\rangle \left\langle g\right| \otimes \mathbb{1} + \Omega \mathbb{1} \otimes \left|r\right\rangle \left\langle g\right| + H.c...) - C_{6,rr}/R^6 \left|rr\right\rangle \left\langle rr\right| \ . \tag{1.15}$$

We can easily make a change of basis to express the dynamics as a three level system with basis $\{|gg\rangle, |+\rangle = (|gr\rangle + |rg\rangle)/\sqrt{2}, |rr\rangle\}$:

$$\hat{H}' = \hbar\sqrt{2}(\Omega \left|gg\right\rangle \left\langle +\right| + \Omega \left|+\right\rangle \left\langle rr\right| + H.c...) - C_{6,rr}/R^6 \left|rr\right\rangle \left\langle rr\right| \ . \tag{1.16}$$

From the structure of the Hamiltonian (1.14), we recognize that in Eq.(1.16) $|gg\rangle$ and $|+\rangle$ are perfectly coupled with a new Rabi frequency $\Omega_0' = \sqrt{2}\Omega_0$, while $|+\rangle$ and $|rr\rangle$ are not, because of the Rydberg-Rydberg interaction. In fact, in complete analogy with Eq. (1.14), this interaction acts as a detuning term decoupling the two states. We can then define the regime of Perfect Blockade as $C_{6,rr}/R_6 \gg \hbar|\Omega_0|$, which corresponds to $R_b := (C_{6,rr}/(\hbar\Omega_0))^{1/6} >> R$ where R_b is the blockade radius. From what we have just said, in this condition $|rr\rangle$ is decoupled from the dynamics as also illustrated in Fig. 1.2.

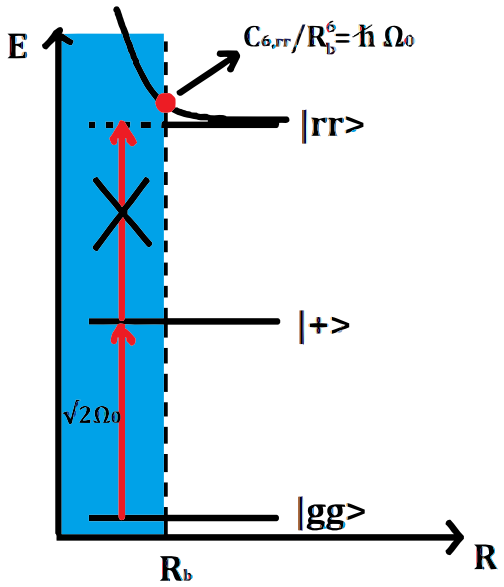

Figure 1.2: The Van der Waals interaction shifts out of resonance the state $|rr\rangle$ if the atoms are separated by $R < R_b$.

Chapter 2

Quantum Optimal Control

Over the last two decades, Quantum Optimal Control has undergone a huge evolution helping the engineering process of quantum physics. Nowadays, this technique is used from control of quantum many-body physics [19] to gate optimization, which is one of the most relevant problems for the realization of digital quantum computers. Quantum optimal control consists of searching for optimal input parameters, which control some physical interaction, in order to achieve a specific objective. The latter is reached by minimizing, or maximizing, a specific objective function. An optimization method to solve the control pulse shaping that evolves a system in the desired manner is the *dressed Chopped Random Basis*(dCRAB) technique [20]. Its features permit to optimize pulses avoiding local minimum, with a natural inclusion of experimental constraints.

In Sec. 2.1 we describe how to fully describe a control problem providing some examples. Then, in Sec. 2.2 we made a brief explanation on the limits of QOC. In Sec. 2.3 we describe CRAB and dCRAB algorithms to optimize pulses in order to control the dynamics of quantum systems.

2.1 Control problems in quantum computing

To define a control problem we need to specify the system dynamics, the objective function to minimize, and the physical constraints we apply [21].

To describe an isolated system we define the Hamiltonian and solve the Schrödinger equation. Moreover, we define a function to minimize that depends on the dynamics and therefore on the control parameters. For example, the simplest optimization problem is the *state to state transfer*, where the objective function J is the infidelity that the initial state ψ_0 evolves after a time T into a chosen state ψ_f:

$$J = 1 - \left|\langle\psi_f|\psi(T)\rangle\right|^2 \ , \tag{2.1}$$

where $|\psi(T)\rangle = U(T,0)\,|\psi_0\rangle$, with time-evolution operator U that depends on control parameters. Minimizing this function over the control parameters corresponds to changing the system dynamics in order to make ψ_0 evolve to the nearest possible state to ψ_f.

In general, one could impose physical constraints in order to implement a more accurate simulation of a real physical system. We will see a specific example where the use of a QOC technique, the CRAB algorithm, naturally imposes a constraint on the bandwidth. Other very useful physical constraints, such as limiting the power of the pulse, are easily

implementable [9] [21].

2.2 Controllability and Quantum Speed Limit

In general, is not always possible to find a QOC solution. We define a quantum system *controllable* if for every unitary transformation on the system there is a control pulse that generates it [22]. It is also necessary that the information stored in the pulse is sufficient to steer the system to the desired state. With information theory arguments it has been shown that, in the noiseless case, the number of degrees of freedom D_r needed to solve a control problem is equal to $D_r = 2N - 2$ where N is the dimension of the quantum system [23]. An intuitive way to see this in the specific case of a state-to-state transfer problem is by considering that the final desired state is described by $2N - 2$ real numbers since we are in an N-dimensional complex Hilbert space with 2 constraints, unitary norm, and independence from the global phase. On top of that, transformations of the system cannot be achieved arbitrarily fast for finite energies. Although time cannot be expressed as a Hermitian operator and hence the general *uncertainty principle* is not applicable for time and energy, we can find bounds for times inversely proportional to energy uncertainty. This is called Quantum Speed Limit (QSL) [24].

2.3 CRAB and dCRAB algorithms

Pulse shaping to drive a specific evolution is a typical control problem and the CRAB and his recursive version dCRAB, proved to be effective and efficient algorithms to face it [19] [20]. Let us consider an isolated system with Hamiltonian $H = H(f(t))$, where f(t) is the control pulse. The main idea of the CRAB algorithm is to make a randomized truncated expansion of the pulse in a given basis, for example in Fourier series, with the coefficients c_i, where i is the base index. The optimization steps for these kind of problems are:

1. Set initial state and coefficients
2. Simulate the dynamics
3. Compute the objective function $J(f(t)) = J(c_1, c_2...c_N)$
4. Update c_i in order to minimize J, and return to step 2.

By setting stopping criteria in the minimization algorithm we conclude our optimization. Note that the minimization algorithm used in the CRAB could be either gradient-free such as Nelder-Mead simplex method algorithm [25], or gradient-based as the GOAT algorithm [26]. Let us consider the pulse $f(t) \in L_2$, where L_2 is the function space of square-integrable

functions. By truncating $f(t)$ in an N basis expansion of L_2 we perform the optimization on a subspace of dimension N risking to consider a local minimum of J as a global one, a so-called false trap. The latter is in fact defined rigorously in the following manner:

$$\delta J(f) = 0 \;\; \forall \; \delta f = \sum_{i=1}^{N} f_i(t)\delta c_i \quad \& \quad \exists \, \delta f \in L_2 : \delta J(f) \neq 0 \tag{2.2}$$

The CRAB algorithm weakens the truncating constraint by choosing randomly the basis functions, e.g. in a Fourier basis the frequencies $c_i = \omega_i$ are chosen stochastically in a fixed interval. One step further to overtake false traps is achievable by introducing the dCRAB. The basic idea is to reiterate the CRAB algorithm each time with an initial pulse equal to the final one of the previous iteration. Those iterations are called super-iteration in order to distinguish them from the ones of the coefficients' optimization. Once we start a new super-iteration the old coefficients do not need to be refreshed because we can consider the old directions of L_2 as already optimized. In fact, in the j-th super-iteration we optimize only $c_i^j, i = 0, 1..N$ of

$$f^j(t) = c_0^j f^{j-1}(t) + \sum_{i=1}^{N} c_i^j f_i^j(t) \;, \tag{2.3}$$

where f^{j-1} is the pulse obtained from the previous one super-iteration and f^j are the new basis functions randomly chosen. As mentioned above, the dCRAB algorithm is very useful to contrast false traps. Supposing we are stuck in one of them, the probability of adding a new random direction and remaining in the false trap is zero because of the infinite possible choices of basis [9].

Despite all the discussion above, the truncation of basis in the CRAB or dCRAB algorithm translates to a natural arise of bandwidth limits which contribute to the capability of these algorithms to encompass experimental constraints [21].

Chapter 3

Quantum computing with neutral atoms

Neutral atoms are one of the most promising platforms to realize digital quantum processors. Encoding qubits in hyperfine ground states permit a long lifetime and weak coupling with surroundings electromagnetic radiation. They are easy to initialize with optical pumping, control with e.m. pulses, and be measured with fluorescence [27]. Furthermore, arrays of identical atoms can be trapped in optical tweezers and their spatial geometry can be easily configured in many ways [28]. The weak interaction between neutral atoms is the key element to trapping a lot of them in a very small volume. However, in that way only one-qubit gates could be realized. By exciting these atoms into Rydberg state we can exploit the Rydberg blockade feature to entangle qubits and then to implement two-qubit gates in order to form a universal quantum computing gate set [4].

In Sec. 3.1 we briefly describe one-qubit gates and simulate them. Then, in Sec. 3.2 and in Sec. 3.3 we explain different protocols for the realization of an ideal CZ gate from [8], [10], [11] implementing and optimizing them in the open-source optimal control suite QuOCS [12]. Quantum optimal control techniques are applied in order to decrease gate infidelity and reduce gate time.

3.1 Single-qubit gate

Let us encode the qubit on two hyperfine ground states of a neutral atom since they are uncoupled to electromagnetic waves in the environment and they have long lifetimes [14]. Single-qubit gates are performed with laser beams that couples the ground state $|0\rangle$ and the excited state $|1\rangle$ with a Rabi frequency Ω_0 and a detuning Δ. The dynamic is described by the Hamiltonian:

$$\hat{H} = \frac{\hbar}{2}\Delta\,|0\rangle\langle 0| - \hbar/2\Delta\,|1\rangle\langle 1| + \hbar(\Omega\,|1\rangle\langle 0| + \Omega^*\,|0\rangle\langle 1|)\ . \tag{3.1}$$

Let us note that this equation is the same as Eq. (1.14) within the sum of a multiple of the identity. If the phase of the pulse is set to zero, we can write the Hamiltonian as a combination of σ_x and σ_z getting as evolution on the Bloch Sphere a rotation around an axis in XZ-plane. If we fix $\Delta = 0$ we get a rotation around the x-axis with frequency Ω, as we see in Fig. 3.1a, while with $\Delta = \Omega_0$ we obtain a rotation around the axis $x + z$ with the same frequency. The latter can be brought back to a Hadamard gate by choosing a pulse time that completes half rotation, as in Fig. 3.1b. Every unitary transformation on a single-qubit can be realized as a combination of Hadamard and X-rotations gates [4].

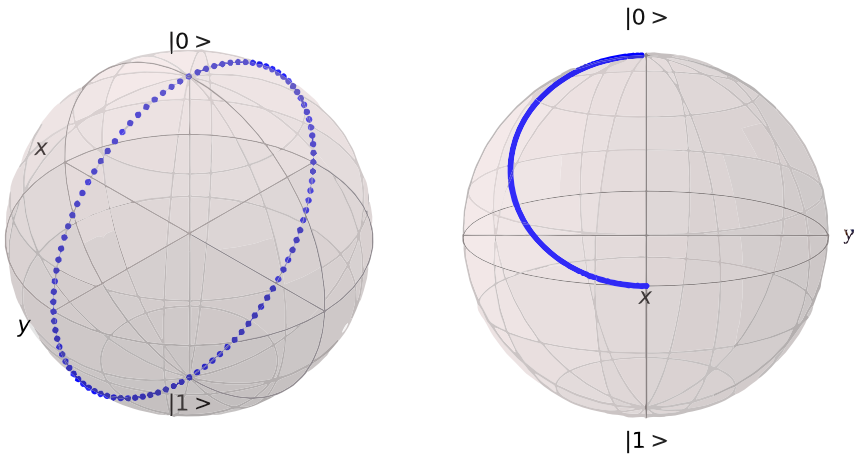

(a) **(b)**

Figure 3.1: *Evolution of* $|0\rangle$ *on the Bloch sphere, simulating one-qubit gates* (a) Simulation with $\Delta = 0$, $\Omega_0 = 10$MHz. By choosing the length of the pulse τ we can make a rotation of an arbitrary angle about the x-axis. In the figure $\tau = 2\pi/\Omega_0$ since Ω_0 is also the frequency of the rotation. (b) Simulation with $\Delta = \Omega_0$, $\Omega_0 = 10MHz$ in order to make an Hadamard gate. The frequency of the rotation is still Ω_0 but the circumference traced has a radius $\sqrt{2}/2$ times smaller than *(a)* and so the pulse time to make a Hadamard gate is $\tau = (\sqrt{2}/2)2\pi/\Omega_0$.

3.2 Two-qubit gate

To make a universal set of gates we need a way to create entangled states, for example with a controlled-phase gate [4]. The latter could be implemented by exploiting the Rydberg Blockade effect in many ways, as shown in Ref. [5] and in [8]. In the following, we will consider two identical atoms, each one modeled as a three-level system with the qubit states $|0\rangle$ and $|1\rangle$ and the Rydberg state $|r\rangle$. The transition between the state $|1\rangle$ and $|r\rangle$ is driven by a detuned laser simultaneously for both atoms. The Hamiltonian is obtained by adding detuning terms to Equation (1.15):

$$H = H_{\Delta=0} + H_{\Delta} \ , \tag{3.2}$$

where $H_{\Delta=0}$ corresponds to Eq. (1.15) and $H_{\Delta} = -\hbar\Delta(|r\rangle\langle r| \otimes \mathbb{1} + \mathbb{1} \otimes |r\rangle\langle r|)$. Since $|0\rangle$ is uncoupled by the laser, the dynamics of $|01\rangle$ can be described in a two-level system $\{|01\rangle, |1r\rangle\}$ with Rabi frequency Ω_0. Instead, as seen in Eq. (1.16), $|11\rangle$ follows a two-level system composed by $\{|11\rangle, \frac{|1r\rangle + |r1\rangle}{\sqrt{2}}\}$ with an enhanced Rabi frequency $\sqrt{2}\Omega_0$. Thanks to different dynamics for $|01\rangle$ and $|11\rangle$, and to the requirement of a laser pulse which guarantees that both states end up in themselves after the evolution, we can make those states acquire different

phases:

$$\begin{aligned} |00\rangle &\rightarrow |00\rangle \\ |01\rangle &\rightarrow |01\rangle\, e^{i\phi_{01}} \\ |10\rangle &\rightarrow |10\rangle\, e^{i\phi_{10}} \\ |11\rangle &\rightarrow |11\rangle\, e^{i\phi_{11}} \ . \end{aligned} \tag{3.3}$$

Where $\phi_{01} = \phi_{10}$ because of the symmetry of their dynamics. If the phases satisfy the relation

$$\phi_{11} = 2\phi_{01} + \pi \ , \tag{3.4}$$

we realize a controlled-Z (CZ) gate, up to a global rotation by ϕ_{01} of the excited state $|1\rangle$.

3.3 Controlled-Z gate optimization

Now, we analyze different protocols for implementing a CZ gate [11]. In particular, we perform a numerical simulation of the two atom system considered in the previous section (Sec. 3.2) and we optimize the gate parameters for a fixed Rabi frequency $\Omega_0 = 10$ MHz. Let us note that this analysis is performed considering an ideal system, i.e. sources of errors like the finite lifetime of the Rydberg state are not introduced. As shown in [11], the leading contribution to the gate infidelity is given by the decay of Rydberg states, which is not taken into account in the evolution of our ideal simulations. The quality of the gate is estimated through a fidelity measurement and in the ideal case we expect at the end of the optimization a fidelity close to 1. To numerically optimize the final phase differences in order to make a CZ gate, we minimize a *state to state* infidelity with initial state $\psi_0 = \dfrac{|01\rangle + |11\rangle}{\sqrt{2}}$ and with target state $\psi_f = \dfrac{|01\rangle + e^{i(\phi_{01}-\pi)}\,|11\rangle}{\sqrt{2}}$. If U(T) is the time evolution operator of our dynamics described by Equation (3.3), the actual expression of the infidelity is:

$$\begin{aligned} J &= 1 - |\,\langle U(T)\psi_0|\psi_f\rangle\,|^2 \\ &= 1 - |(e^{i\phi_{01}}\frac{|01\rangle + e^{i(\phi_{11}-\phi_{01})}\,|11\rangle}{\sqrt{2}}) \cdot (\frac{|01\rangle + e^{i(\phi_{01}-\pi)}\,|11\rangle}{\sqrt{2}})|^2 \ . \end{aligned} \tag{3.5}$$

We then see that J has a global minimum if the condition given by Eq. (3.4) is fulfilled. Note that J is the same as a Bell state infidelity within perfect single-qubit gates transformation.
In the Subsection 3.3 we reproduce the protocol of [8], with two laser pulses of length τ, phase jump ξ and constant detuning Δ, in the hypothesis of perfect blockade. Then, we optimize the detuning and the gate time in the imperfect blockade regime analyzing its impact on the dynamics and on the gate time. In the Subsection 3.3, we apply optimal quantum control on a symmetric detuning pulse $\Delta(t)$ with a zero phase, in order to reduce the gate time τ' and the

infidelity.

Constant detuning with phase jump

Let us assume a perfect Rydberg blockade, i.e. with the state $|rr\rangle$ decoupled from the dynamics. In this case, an analytical solution that fulfills the pulse contraints exists [8], thus we do not perform any numerical optimization. We consider two pulses of length $\tau = 2\pi/\sqrt{\Delta^2 + 2\Omega_0^2}$ chosen in a way that $|11\rangle$ undergoes a complete rotation in the Bloch sphere, gaining a phase $\phi_{11}/2$. This behavior is shown in Fig. 3.2b. Note that $|01\rangle$ does not make a complete oscillation after the first pulse since its dynamics has not an enhanced Rabi Frequency as $|11\rangle$. However, by a proper choice of the phase jump ξ, as indicated in [8], we can guarantee that after the second pulse the state $|01\rangle$ returns to himself with a dynamical phase ϕ_{01}, as we see in Fig. 3.2a. Both ϕ_{01} and ϕ_{11} can be expressed analytically as function of Δ/Ω, and from the phases constraint of Eq. (3.4) we get the relation $\Delta/\Omega_0 = 0.377$. Then, we are able to obtain all the remaining parameters, as indicated in Table 3.1a.

Let us now consider the imperfect Rydberg blockade case. In particular, let us consider

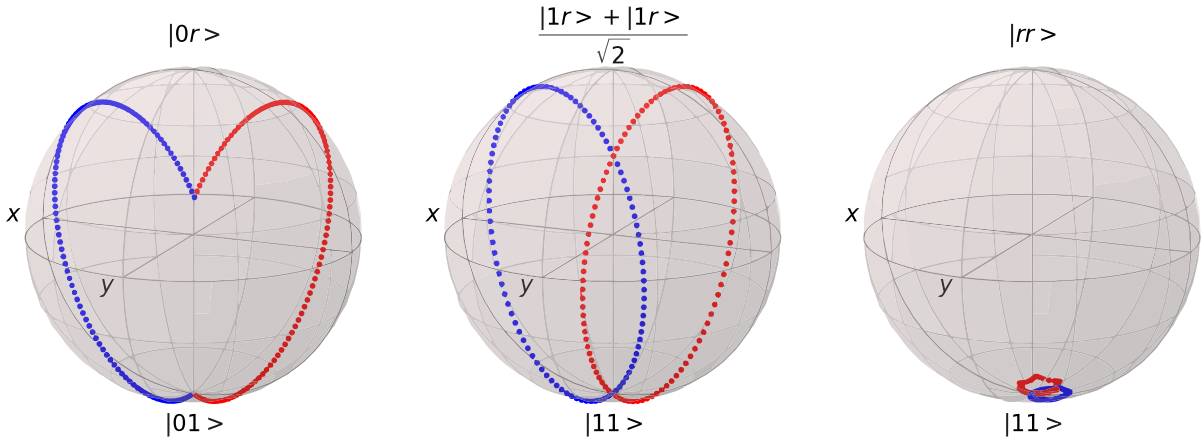

Figure 3.2: *Evolution of states $|01\rangle$, $|11\rangle$ on the Bloch sphere in the imperfect blockade regime, with constant detuning and a phase jump between the two pulses. For the first two Bloch-spheres, a perfect blockade regime is visually the same.* (a) The phase jump ξ changes the axis of rotation symmetrically making return $|01\rangle$ in itself with a phase $|\phi_{01}\rangle$. (b) The length of each pulse τ is chosen such that $|11\rangle$ undergoes a complete rotation acquiring a phase $\phi_{11}/2$. (c) The percentage in the evolution of $|11\rangle$ composed by $|rr\rangle$ is negligible and so its contribution to the Rydberg states decay probability.

two Strontium-88 atoms at an interatomic distance of 3um [29]. The imperfect blockade term seen in Sec. 1.2 affects only the dynamic of $|11\rangle$ and then we can keep the expression of ξ to guarantee a complete rotation of $|01\rangle$ after the two pulses. Furthermore, we can always

Parameters	Ω_0	ξ	τ	Δ	$V/\hbar$	J
Value	10 MHz	3.90	0.43 μs	3.77 MHz	∞	$3.5 \cdot 10^{-6}$

(a) Perfect blockade regime

Parameters	Ω_0	ξ	τ	Δ	$V/\hbar$	J
Value	10 MHz	3.93	0.43 μs	3.91 MHz	211 MHz	$7 \cdot 10^{-6}$

(b) Imperfect blockade regime

Table 3.1: Input parameters and results of the simulation of a protocol with constant detuning and a phase jump.

choose τ such that the $|11\rangle$ makes a closed path in the Bloch Sphere, and then we can use Δ as a control knob to adjust the right dynamical phases between $|01\rangle$ and $|11\rangle$ [8]. The detuning and the gate time of the pulses are now optimized by using the direct search method of Nelder-Mead to minimize infidelity in Eq.(3.5). As we can see in Table 3.1, ξ and Δ slightly change in different regimes, but without visible variation of trajectories on the Bloch Sphere for states $|01\rangle$, as seen in Fig. 3.2a, and $|11\rangle$ in Fig. 3.2b. During the evolution of $|11\rangle$ only a very small percentage of $|rr\rangle$ is present, as we can see in Fig. 3.2c. This means that the average time passed on a Rydberg state is practically the same for the two regimes and so the decay probability of those states [11].

One can demonstrate that a protocol with time-dependent phase of the laser $\xi(t)$ and constant detuning Δ is equivalent, within a unitary transformation, to a protocol with time-dependent detuning $\Delta(t)$ with the form of $\Delta(t) = \Delta + \dot{\xi}(t)$ and with zero phase [10]. Then, if we view the protocol analysed above with an Heaviside function $\xi(t) = H(t - \tau)$ with the step after the first pulse, the system is equivalent to a protocol with $\Delta(t) = \Delta + \delta(t - \tau)$. Because of that equivalence, from now on we will only consider protocols composed of one single pulse with time-dependent detuning and a zero phase.

Detuning optimization with dCRAB

We now apply the dCRAB algorithm, with settings reported in Figure 3.3, to improve the gate performance. We optimize the detuning pulse $\Delta(t)$ while changing in a fixed range the gate time to find its minimum duration τ'. Let us note that according to the quantum speed limit, a minimum value of tau exist since we are working with a finite power pulse. Since here we cannot apply the analytical constraints found before to make $|01\rangle$ and $|11\rangle$ back to themselves, we have to operate differently. For a fixed time of the pulse and with the constraint of a symmetric $\Delta(t)$, the optimization algorithm needs to find a first half of the detuning which is able to make both states evolve into a point of the XZ plane in the Bloch-sphere space. Indeed with a time-dependent Hamiltonian, the evolution on a Bloch

sphere is a series of infinitesimal rotations around different axes that belong to the XZ-plane, since the Hamiltonian at each time can be decomposed in a sum of σ_x and σ_z. Then, if after a time $\tau'/2$ the states evolved on an XZ-plane point, we are sure that they will return to themselves after another $\tau'/2$ because of the symmetry of the detuning and the fact that the rotations are around axes on the XZ plane. That is confirmed by our simulations as we can see in Fig. 3.3a and in Fig. 3.3b. The optimization brings to the pulse in Fig. 3.3c which

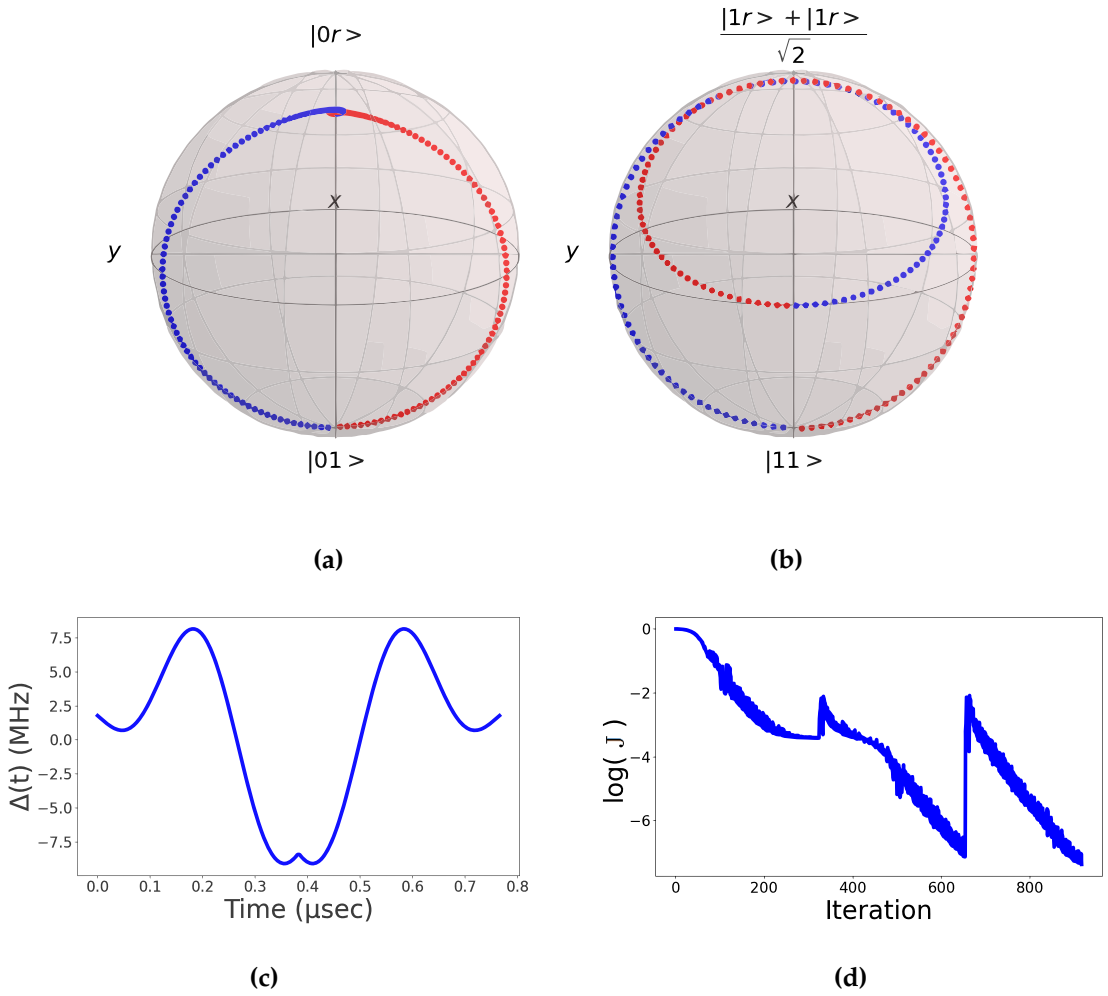

Figure 3.3: *Analysis of the realization of a CZ gate with a time-dependent detuning optimized with the dCRAB Algorithm* (a,b) Evolution of states $|01\rangle$, $|11\rangle$ on the Bloch sphere. After $\tau'/2$ the state evolved in the XZ plan in such a way that can return to itself after another $\tau'/2$. (c,d) Control pulse and Figure of merit(objective function) after an optimization with the dCRAB method using the Nelder-Mead algorithm. We use 4 vectors in the Fourier basis with random uniform distribution picked in the interval [0, 1.6 MHz]. We do 3 super-iterations with a maximum of 500 evaluations each.

reduce the gate time by 10%, as we can see in Table 3.2. This improvement is very useful since it has been established that the biggest contribution to infidelity is given by medium

Parameters	Ω_0	$\tau'/2$	$V/\hbar$	J
Value	10 MHz	0.385 μs	211 MHz	$4.1 \cdot 10^{-8}$

Table 3.2: Input parameters and results of the simulation of a protocol with time-dependent detuning optimized with the dCRAB algorithm

time passed on a Rydberg state which decreases with gate time [11].

Now, we analyze how the interatomic distance r affects the minimum gate time possible, which exists in accordance with QSL. We set a threshold of 10^{-6} on the infidelity to consider if an optimization converges or not. For $r > 4\mu$m the optimization does not converge, while for

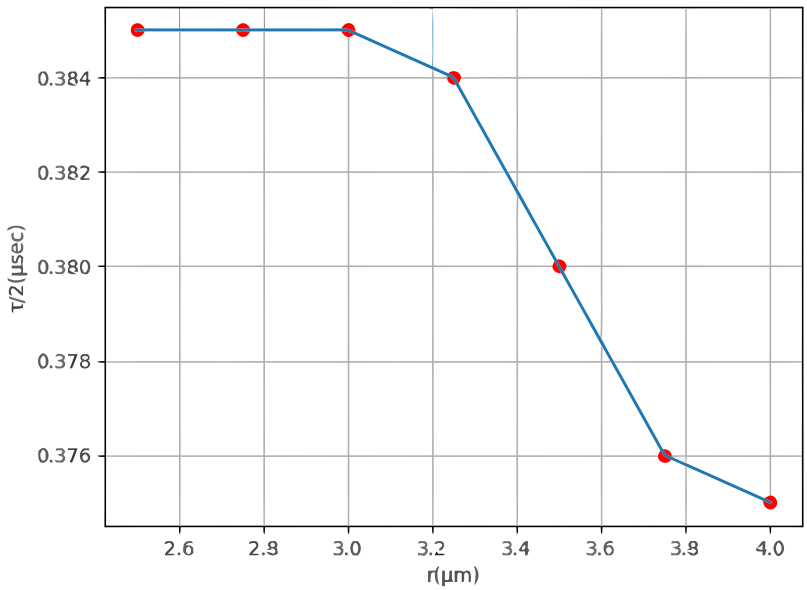

Figure 3.4: Plot of half gate time $\tau'/2$ as a function of the interatomic distance r of two strontium-88 atoms. For each interatomic distance, τ' is the minimum accessible gate duration in accordance with QSL.

$r < 3\mu$m the gate time quickly tends towards a perfect blockade regime. As shown in Fig. 3.4, in the range $r \in [3, 4]\mu$m, we see that the gate time decrease with the interatomic distance. At a distance r of 4μm we find an half duration of the pulse of $\tau'/2 = 0.375\mu$s. Then, we can loosen r in order to obtain a smaller gate time and then a better realistic gate fidelity.

Conclusion

In this Thesis, we have shown applications of Quantum Optimal Control techniques for the implementation of a controlled-phase gate in a Rydberg atoms quantum computer. Firstly, we have reviewed the general properties of Rydberg atoms and their interactions, with a particular focus on the Rydberg blockade. Then, we have introduced the basic concepts of QOC theory, summarizing the *dressed Chopped Random Basis* (dCRAB) algorithm and its capability of avoiding false traps in comparison to the CRAB algorithm.

We have shown how to implement one-qubit gates in a Rydberg atoms device. We have simulated the one-qubit Hamiltonian to reproduce the behavior of Hadamard and X-rotation gates. Indeed, by combining those gates it is possible to realize any one-qubit rotation. To obtain a universal gate set, entangling operations are required. Thus, we have reviewed some protocols to implement a controlled-Z gate in the neutral atoms platform. For this purpose, we have simulated the Hamiltonian of a system of two identical Rydberg atoms driven by a laser field that couples the excited state $|1\rangle$ to the Rydberg state $|r\rangle$. To reproduce the behavior of a controlled-Z gate, we have first analyzed the case of two laser pulses of time length τ with constant detuning Δ and a phase jump ξ between them, in the case of perfect Rydberg blockade. By fixing a Rabi frequency of $\Omega_0 = 10$MHz, we obtain an optimal pulse length $\tau = 0.43\mu$s with the laser detuned by $\Delta = 3.77$MHz. We have studied also the case of a finite Rydberg interaction. In particular, we suppose to have two strontium-88 atoms at an interatomic distance of 3μm. In this case, we fix the interaction $V = 211$MHz and we find that the optimal pulse length is still $\tau = 0.43\mu s$ with approximately the same detuning of the perfect blockade case.

Afterwards, since it can be shown that this protocol is equivalent to one with a zero phase and a time-dependent detuning $\Delta(t)$, we consider only the last one to verify if with an optimal control optimization we can reduce the gate time τ'. Accordingly to Ref. [11], we have obtained a reduction of the gate time of about 10% finding $\tau'/2 = 0.385\mu$s. The reduction in pulse length is a great improvement since the total duration of the pulse is directly related to the time spent in the Rydberg state. The decay out of the Rydberg state is the main source of intrinsic errors in a Rydberg platform and thus minimizing the time in this state can increase the quality of the gate operation. We further investigate this protocol by analyzing the dependence of the minimum gate time achievable with the interatomic distance between the two atoms. We see that, for a distance $r < 3\mu$m, the gate time very quickly tends towards the value found in the perfect blockade regime, and for $r > 4\mu$m, a solution cannot be found anymore due to the weak interaction. However, in the range $r \in [3, 4]\mu$m, we can always find a solution in which the gate time turns out to be inversely proportional to interatomic distance. At a distance of $r = 4\mu$m, we find an optimal half duration of the gate of

$\tau'/2 = 0.375\mu$s.

In conclusion, we have reproduced the results of Refs. [8] and [11]. We have made an extensively use of optimal control techniques, as implemented in QuOCS [12], showing their capability of improving gate quality in a Rydberg atoms quantum device.

Bibliography

[1] R. P. Feynman, "Simulating physics with computers," *International journal of theoretical physics*, vol. 21, no. 6/7, pp. 467–488, 1982.

[2] P. W. Shor, "Polynomial-time algorithms for prime factorization and discrete logarithms on a quantum computer," *SIAM Journal on Computing*, vol. 26, pp. 1484–1509, oct 1997.

[3] C. Moore, D. Rockmore, and A. Russell, "Generic quantum fourier transforms," *ACM Trans. Algorithms*, vol. 2, p. 707–723, oct 2006.

[4] M. A. Nielsen and I. L. Chuang, *Quantum Computation and Quantum Information: 10th Anniversary Edition*. Cambridge University Press, 2010.

[5] D. Jaksch, J. I. Cirac, P. Zoller, S. L. Rolston, R. Côté, and M. D. Lukin, "Fast quantum gates for neutral atoms," *Phys. Rev. Lett.*, vol. 85, pp. 2208–2211, Sep 2000.

[6] T. F. Gallagher, *Rydberg Atoms*. Cambridge Monographs on Atomic, Molecular and Chemical Physics, Cambridge University Press, 1994.

[7] A. Ashkin, "Optical trapping and manipulation of neutral particles using lasers," *Proceedings of the National Academy of Sciences*, vol. 94, no. 10, pp. 4853–4860, 1997.

[8] H. Levine, A. Keesling, G. Semeghini, A. Omran, T. T. Wang, S. Ebadi, H. Bernien, M. Greiner, V. Vuletić , H. Pichler, and M. D. Lukin, "Parallel implementation of high-fidelity multiqubit gates with neutral atoms," *Physical Review Letters*, vol. 123, oct 2019.

[9] M. M. Müller, R. S. Said, F. Jelezko, T. Calarco, and S. Montangero, "One decade of quantum optimal control in the chopped random basis," *Reports on Progress in Physics*, vol. 85, p. 076001, jun 2022.

[10] A. Pagano, "Optimal quantum gates for rydberg atoms quantum computer," *Master thesis: https://thesis.unipd.it/browse?type=authorauthority=st766495*, 2021.

[11] A. Pagano, S. Weber, D. Jaschke, T. Pfau, F. Meinert, S. Montangero, and H. P. Büchler, "Error budgeting for a controlled-phase gate with strontium-88 rydberg atoms," *Physical Review Research*, vol. 4, jul 2022.

[12] M. Rossignolo, A. Marshall, T. Reisser, P. Rembold, A. Pagano, P. Vetter, R. Said, M. Müller, T. Calarco, S. Montangero, and F. Jelezko, "QuOCS: Quantum Optimal Control Suite." *GitHub*, `https://github.com/Quantum-OCS/QuOCS`, 2021.

[13] C. S. Adams, J. D. Pritchard, and J. P. Shaffer, "Rydberg atom quantum technologies," *Journal of Physics B: Atomic, Molecular and Optical Physics*, vol. 53, p. 012002, dec 2019.

[14] X. Wu, X. Liang, Y. Tian, F. Yang, C. Chen, Y.-C. Liu, M. K. Tey, and L. You, "A concise review of rydberg atom based quantum computation and quantum simulation," *Chinese Physics B*, vol. 30, p. 020305, feb 2021.

[15] R. Brooks, *The Fundamentals of Atomic and Molecular Physics*. Undergraduate Lecture Notes in Physics, Springer New York, 2014.

[16] S. Weber, C. Tresp, H. Menke, A. Urvoy, O. Firstenberg, H. P. Büchler, and S. Hofferberth, "Calculation of rydberg interaction potentials," *Journal of Physics B: Atomic, Molecular and Optical Physics*, vol. 50, p. 133001, jun 2017.

[17] J. Nipper and T. Pfau, *Interacting Rydberg Atoms: Coherent Control at Förster Resonances and Polar Homonuclear Molecules*. Universitätsbibliothek der Universität Stuttgart, 2012.

[18] Y. Wu and X. Yang, "Strong-coupling theory of periodically driven two-level systems," *Phys. Rev. Lett.*, vol. 98, p. 013601, Jan 2007.

[19] P. Doria, T. Calarco, and S. Montangero, "Optimal control technique for many-body quantum dynamics," *Physical Review Letters*, vol. 106, may 2011.

[20] T. Caneva, T. Calarco, and S. Montangero, "Chopped random-basis quantum optimization," *Physical Review A*, vol. 84, aug 2011.

[21] P. Rembold, N. Oshnik, M. M. Müller, S. Montangero, T. Calarco, and E. Neu, "Introduction to quantum optimal control for quantum sensing with nitrogen-vacancy centers in diamond," *AVS Quantum Science*, vol. 2, p. 024701, jun 2020.

[22] D. D'Alessandro, *Introduction to Quantum Control and Dynamics*. Chapman & Hall/CRC Applied Mathematics & Nonlinear Science, CRC Press, 2007.

[23] S. Lloyd and S. Montangero, "Information theoretical analysis of quantum optimal control," *Physical Review Letters*, vol. 113, jul 2014.

[24] S. Deffner and S. Campbell, "Quantum speed limits: from heisenberg's uncertainty principle to optimal quantum control," *Journal of Physics A: Mathematical and Theoretical*, vol. 50, p. 453001, oct 2017.

[25] J. A. Nelder and R. Mead, "A simplex method for function minimization," *Computer Journal*, vol. 7, pp. 308–313, 1965.

[26] S. Machnes, E. Assémat, D. Tannor, and F. K. Wilhelm, "Tunable, flexible, and efficient optimization of control pulses for practical qubits," *Phys. Rev. Lett.*, vol. 120, p. 150401, Apr 2018.

[27] L. Henriet, L. Beguin, A. Signoles, T. Lahaye, A. Browaeys, G.-O. Reymond, and C. Jurczak, "Quantum computing with neutral atoms," *Quantum*, vol. 4, p. 327, sep 2020.

[28] D. Barredo, V. Lienhard, S. de Léséleuc, T. Lahaye, and A. Browaeys, "Synthetic three-dimensional atomic structures assembled atom by atom," *Nature*, vol. 561, pp. 79–82, sep 2018.

[29] J. Mitroy and M. Bromley, "Semiempirical calculation of van der waals coefficients for alkali-metal and alkaline-earth-metal atoms," *Physical Review A*, vol. 68, no. 5, pp. 52714.1–52714.16, 2003.